Contract No:

This document was prepared in conjunction with work accomplished under Contract No. 89303321CEM000080 with the U.S. Department of Energy (DOE) Office of Environmental Management (EM).

Disclaimer:

This work was prepared under an agreement with and funded by the U.S. Government. Neither the U.S. Government or its employees, nor any of its contractors, subcontractors or their employees, makes any express or implied:

1) warranty or assumes any legal liability for the accuracy, completeness, or for the use or results of such use of any information, product, or process disclosed; or
2) representation that such use or results of such use would not infringe privately owned rights; or
3) endorsement or recommendation of any specifically identified commercial product, process, or service.

Any views and opinions of authors expressed in this work do not necessarily state or reflect those of the United States Government, or its contractors, or subcontractors.

Recombination of Hydrogen in the Iodine Reactors

K. M. L. Taylor-Pashow

J. M. Gogolski

M. L. Restivo

J. M. Pareizs

W. E. Daniel

T. S. Rudisill

DISCLAIMER

Recombination of Hydrogen in the Iodine Reactors

K. M. L. Taylor-Pashow
J. M. Gogolski
M. L. Restivo
J. M. Pareizs
W. E. Daniel
T. S. Rudisill

November 2021

Savannah River National Laboratory®

REVIEWS AND APPROVALS

AUTHORS:

_____

K. M. L. Taylor-Pashow, Separation Sciences and Engineering   Date

_____

J. M. Gogolski, Actinide and Separations Science   Date

_____

M. L. Restivo, Separation Sciences and Engineering   Date

_____

J. M. Pareizs, Chemical Flowsheet Development   Date

_____

W. E. Daniel, Actinide and Separations Science   Date

_____

T. S. Rudisill, Actinide and Separations Science   Date

TECHNICAL REVIEW:

_____

H. W. Eldridge, Actinide and Separations Science, Reviewed per E7 2.60   Date

APPROVAL:

_____

B. J. Wiedenman, Manager   Date
Separation Sciences and Engineering

_____

J. M. Duffey, Manager   Date
Actinide and Separations Science

_____
F. M. Pennebaker, Director, Chemical Processing   Date

_____
A. M. Hudlow, SRNS Materials Disposition Engineering   Date

ACKNOWLEDGEMENTS

EXECUTIVE SUMMARY

The H-Canyon facility is currently dissolving spent nuclear fuel, including Material Test Reactor (MTR) and High Flux Isotope Reactor (HFIR) fuel. Dissolution of aluminum spent nuclear fuel produces hydrogen and other NOx gases. A theory long held by H-Canyon Engineering and Facility Technical Advisors that the silver nitrate-coated berl saddles, present in the iodine reactor, used for off-gas treatment were acting as a catalytic hydrogen recombiner was captured during an external review of the Accelerated Basin De-inventory program. Results from a separate SRNL project using a Raman Spectrometer to monitor the off-gas from the dissolution process indicated a lack of the expected hydrogen in the off-gas stream. To test this hypothesis, a laboratory scale iodine reactor was assembled and filled with silver nitrate-coated berl saddles. Testing with this laboratory scale reactor confirmed the recombination of hydrogen when a simulated dissolver off-gas was passed through the reactor containing silver nitrate-coated berl saddles at 173-188 °C. Control experiments performed with uncoated berl saddles resulted in no change to the hydrogen concentration after passing through the reactor.

The residence time of the gas in the reactor was varied to determine if residence time had an impact on the amount of hydrogen recombination occurring. Results from these experiments indicated that at the shortest residence times tested (~5 seconds) recombination of the hydrogen still exceeded 90%; however, the percent recombination did increase at longer residence times, reaching 97.9% or greater for residence times over 10 seconds.

Finally, testing performed with a simplified off-gas composition containing only hydrogen and air gave similar results, indicating that the presence of NO and N_2O gases in the stream do not play a role in the recombination reaction.

TABLE OF CONTENTS

LIST OF TABLES

LIST OF FIGURES

LIST OF ABBREVIATIONS

ABD	Accelerated Basin De-inventory
ASNF	aluminum spent nuclear fuel
DACS	data acquisition and control system
DI	deionized water
EDL	Engineering Development Lab
ELN	Electronic Laboratory Notebook
FCA	Fast Critical Assembly
GC	gas chromatograph
HFIR	High Flux Isotope Reactor
LFL	Lower Flammability Limit
M&TE	measurement and test equipment
MS&E	measurement systems and equipment
MTR	Material Test Reactor
NFPA	National Fire Protection Association
NIST	National Institute of Standards and Technology
SRNL	Savannah River National Laboratory
SRS	Savannah River Site
STP	standard temperature and pressure
TTQAP	Task Technical and Quality Assurance Plan
TTR	Task Technical Request

1.0 Introduction

The H-Canyon facility at the Savannah River Site (SRS) is currently dissolving aluminum spent nuclear fuel (ASNF) that has been stored in L-Area Facility Basin. Two fuel types are currently being dissolved, Material Test Reactor (MTR) and High Flux Isotope Reactor (HFIR) fuel. An external review conducted in support of the Accelerated Basin De-inventory (ABD) program, suggested the silver nitrate-coated berl saddles, present in the iodine reactors, used for off-gas treatment may be acting as a catalytic hydrogen recombiner.

In H-Canyon, the ASNF is chemically dissolved in a solution of nitric acid with mercuric nitrate added as a catalyst.[1,2] The composite reactions representing the dissolution are shown in Equations 1 and 2 below[3]:

$$Al + 3.75HNO_3 \xrightarrow{Hg^{2+}} Al(NO_3)_3 + 0.225NO + 0.15N_2O + 0.11N_2 + 1.9H_2O + 190\frac{kcal}{mole\ Al} \quad (1)$$

$$U + 4HNO_3 \rightarrow UO_2(NO_3)_2 + 2NO + 2H_2O \quad (2)$$
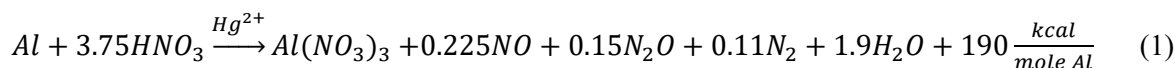
The mercury catalyzed dissolution of aluminum in nitric acid produces a number of off-gas species including NO_2, NO, N_2O, N_2, and H_2 through the following reactions[4]:

$$Al + 6HNO_3 \rightarrow Al(NO_3)_3 + 3NO_2 + 3H_2O \quad (3)$$

$$Al + 4HNO_3 \rightarrow Al(NO_3)_3 + NO + 2H_2O \quad (4)$$

$$8Al + 30HNO_3 \rightarrow 8Al(NO_3)_3 + 3N_2O + 15H_2O \quad (5)$$

$$10Al + 36HNO_3 \rightarrow 10Al(NO_3)_3 + 3N_2 + 18H_2O \quad (6)$$

$$2Al + 6HNO_3 \rightarrow 2Al(NO_3)_3 + 3H_2 \quad (7)$$
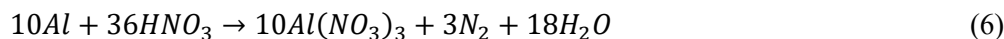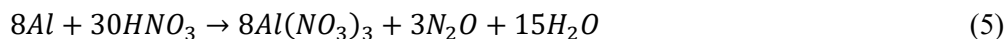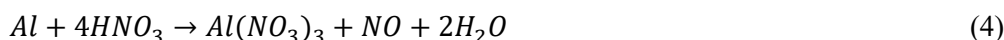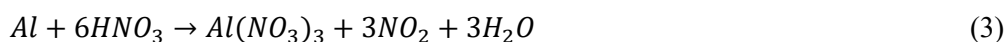
The off-gas that is generated during the dissolution passes first through a condenser which serves to recover the nitric acid through conversion of the NO_x gases. It is then routed through a heated iodine reactor which is packed with silver nitrate-coated berl saddles. This reactor is maintained at a temperature of 173 to 188 °C and is designed to trap radioactive iodine. After leaving the iodine reactor, the off-gas passes through a particulate filter prior to being emitted from the stack. During the development of this task to study the hydrogen recombining hypothesis, a Raman spectrometer deployed by Savannah River National Laboratory (SRNL) to monitor the off-gas from the dissolution of the ASNF did not detect hydrogen.[5] The Raman spectrometer sampling point is located after the particulate filter. Early data from development and testing of the Raman spectrometer was inconsistent with expectations, giving further merit to this hypothesis. This study was then established to investigate the theory that the silver nitrate-coated berl saddles in the iodine reactor were acting as a catalytic hydrogen recombiner and to provide increased understanding of the H-Canyon facility chemistry.

2.0 Experimental Procedure

2.1 Preparation of Berl Saddles

Unglazed porcelain berl saddles (obtained from Chemglass Life Sciences) with an outer diameter of 8 mm were coated with silver nitrate (AgNO₃, 99.9% purity from Alfa Aesar) using the following procedure. A batch of berl saddles (~29 g) was immersed in a 13-14 M solution of silver nitrate for three minutes at 82 °C. The berl saddles were contained in a borosilicate perforated basket made by the SRNL Glass Shop. The

solution was constantly mixed using a magnetic stir bar. The solution density was periodically checked to ensure it remained within the desired range of 2.2 – 2.4 g/mL.[6,7] The solution density was adjusted with either additional deionized (DI) water or AgNO$_3$, as needed. After removal of the berl saddles from solution, they were rinsed with DI water to remove excess AgNO$_3$. The berl saddles were air dried for several minutes before being patted dry. The berl saddles were then placed in an electric oven set to 121 °C for six hours. Once the berl saddles were completely dry, the weight percent (wt %) increase was determined to confirm AgNO$_3$ deposition on the berl saddles. A total of 10 batches were prepared and were combined after determining the final mass of each batch. The berl saddles were stored in an airtight container placed in a cool and dark location before use in the reactor.

2.2 Laboratory Scale Iodine Reactor and Gas System

A laboratory scale set-up modeling the gas flow through the H-Canyon iodine reactor was assembled in the Engineering Development Lab (EDL) of SRNL. The set-up included gas cylinders supplying hydrogen (H$_2$), nitric oxide (NO), and nitrous oxide (N$_2$O) which are the main components of the off-gas generated from the dissolution of ASNF in nitric acid. The air was supplied from plant air plumbed into the hood. All gas flows were set and monitored using MKS mass flow controllers and ¼" stainless steel tubing was used for the gas lines, except for hydrogen which utilized 1/8" tubing. The mass flow controllers were all calibrated at 70 °F with the exception of the one used for NO, which was calibrated at 0 °C. The NO data was corrected to 70 °F at the conclusion of the experiments. The individual gases were mixed using an inline Koflo Model PN ¼-21 static mixer before entering the first furnace. The gas line was coiled inside of the first furnace to extend the residence time allowing for heating of the gas prior to entering the iodine reactor. The iodine reactor was positioned vertically inside a second tube furnace. The reactor was fabricated from stainless steel tubing with a nominal inside diameter of 1.23". The total length of the reactor was 18" (interior dimension); however, the bed length (packed with berl saddles) was nominally 8". A photograph of the reactor vessel is shown in Figure 2-1. A stainless steel insert was used to position the start of the bed approximately 5" above the bottom of the tube. Figure 2-2 shows the insert used to position the bed and a photograph of the saddles inside the reactor. Four Type-K thermocouples were used to monitor temperatures at the following locations: prior to entering the first furnace (after the static mixer); between the first and second furnaces; in the berl saddle reactor bed; and upon exiting the reactor. The furnaces were set to control the temperature of the reactor vessel bed to 173 – 188 °C. A full list of equipment used is provided in Appendix A.
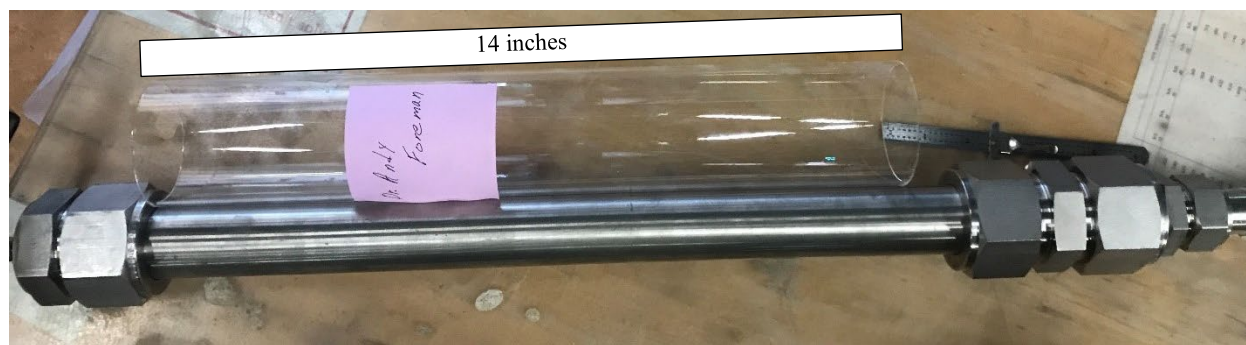
Figure 2-1. Photograph of the lab scale iodine reactor. The adjacent glass tube was used to ensure there was no contact with the heating elements when the reactor was placed into the furnace.

Figure 2-2. Photographs of the insert used to position berl saddle bed in the reactor (left) and berl saddles loaded into the reactor (right).

The test parameters required the use of hydrogen above 25% of the Lower Flammability Limit (LFL) (LFL is ~4% H_2 at STP). Measurement and Test Equipment (M&TE) calibrated mass flow controllers on all gases were used to allow constant monitoring of the concentration of hydrogen under all flow conditions. During experiments, a readout was provided of the instantaneous percent hydrogen concentration, and the computer would shut down H_2 (only) flow when the preset setpoint (60% of the LFL) was violated. This stopped all hydrogen flow while allowing continuation of all other gases, purging the system immediately of excess hydrogen. Figure 2-3 provides a photograph of the Data Acquisition and Control System (DACS) screen where flow rates are entered, and hydrogen concentration is calculated and displayed. This system was verified before testing.
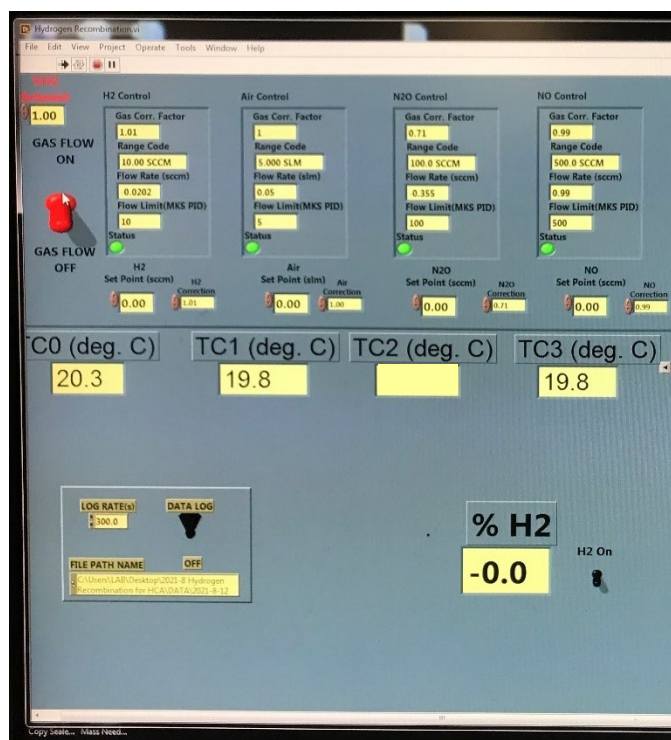
Figure 2-3. Data Acquisition and Control System Screen.

A Micro GC (gas chromatograph) Fusion® Gas Analyzer was used to measure the hydrogen concentration in the gas stream both upstream (feed) and downstream (outlet) of the reactor. Stainless steel tubing (1/16") was run from just after the static mixer as well as from the outlet of the reactor to the GC; valves were also installed to isolate these two slip streams. A schematic of the set-up is provided in Figure 2-4 and a photograph of the set-up is provided in Figure 2-5.
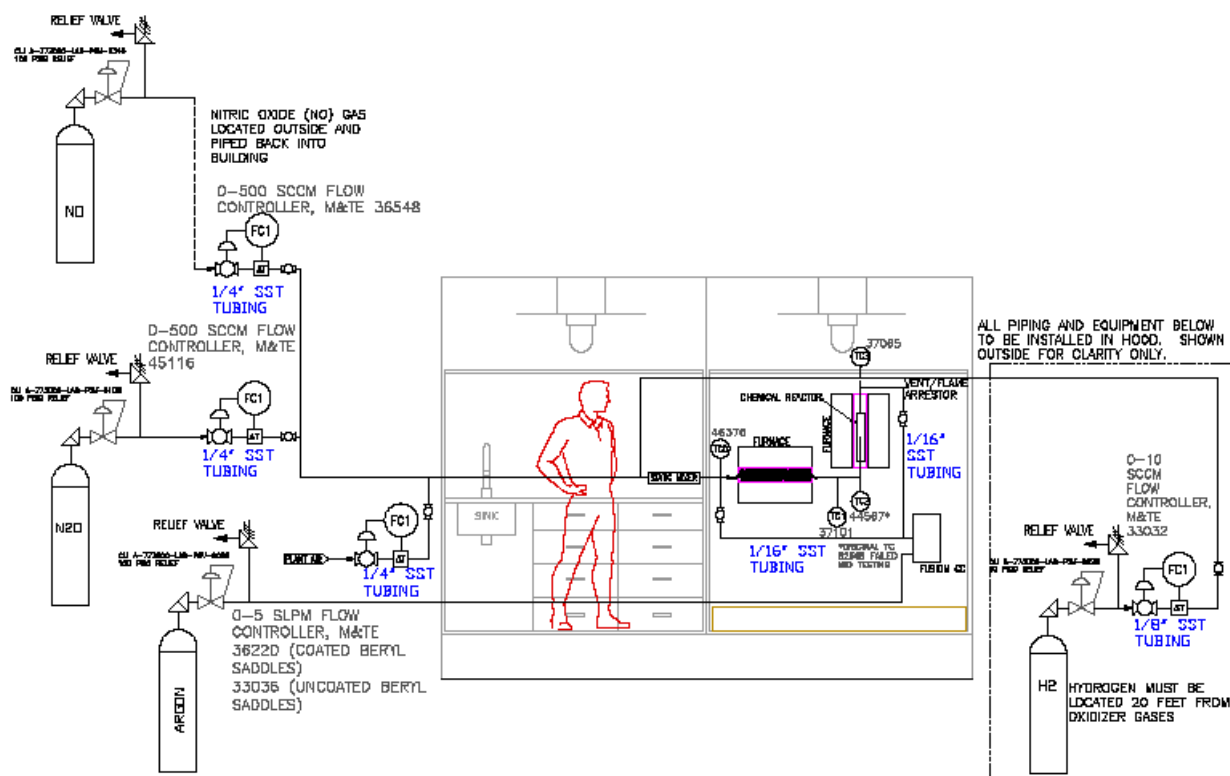
Figure 2-4. Piping and Instrument Diagram of Testing Set-up.
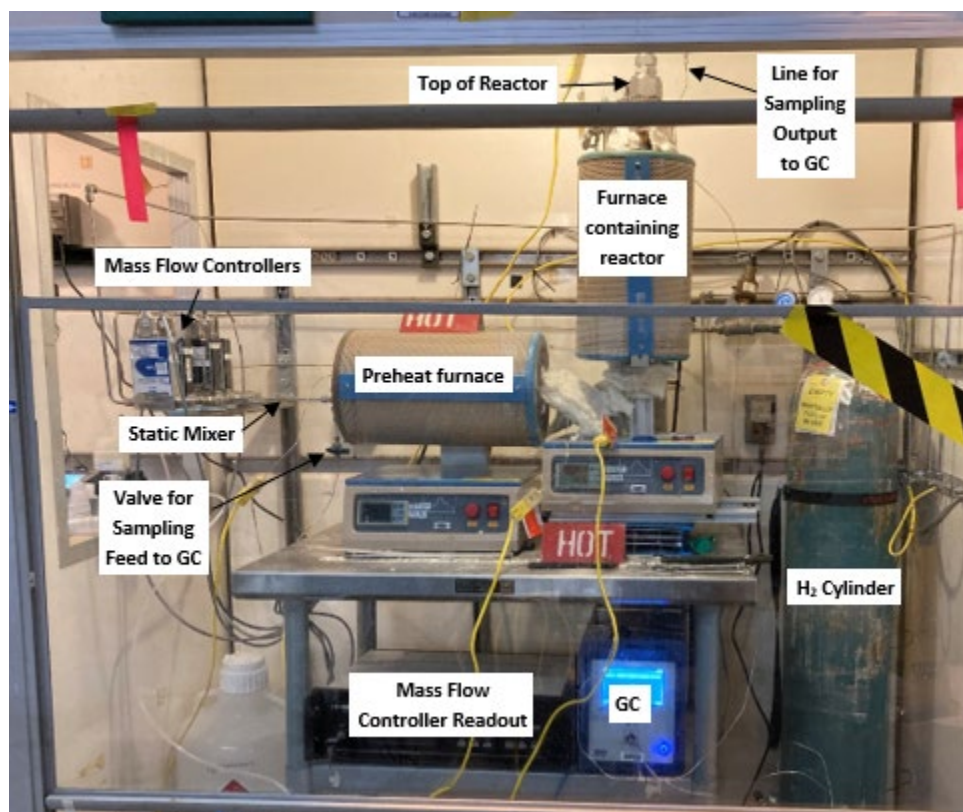
Figure 2-5. Labeled Photo of Set-up.

2.3 <u>Gas Chromatography Calibration</u>

The off-gas was analyzed with a dual channel Fusion® micro gas chromatograph (GC). The GC is part of the Measurement Systems and Equipment (MS&E) program and its use is governed by procedure.[8] Channel A was equipped with a Molsieve 5A column and was used to quantify hydrogen. Channel B contained a Q-Bond column for quantification of N_2O. The gases have different affinities for the column materials, resulting in separation (varying retention time), allowing for quantification of individual gases. Both channels utilized a thermal conductivity detector. The Micro GC Fusion® Gas Analyzer was calibrated with NIST traceable calibration gases at three different hydrogen concentrations, 3%, 1.5%, and 0.5% H_2. The balance of the gas was made up of a mixture of N_2O, oxygen and nitrogen. NO cannot be quantified via GC, and therefore it was omitted from the calibration gases. The density of this gas, a factor in this instrument's response, is similar to air and therefore its omission was not expected to have a significant impact on the calibration and measurement of H_2 in this matrix. The average concentration of the N_2O in the feed test matrix was used for calibration gases 1 and 2, but at the request of the vendor this amount was decreased to 5.0% for the third calibration gas. For the lower hydrogen concentrations (0.5% and 1.5%), the oxygen and nitrogen composition was that of air; however, for the third calibration gas (3% H_2) the balance of air was replaced with a balance of nitrogen, again at the request of the vendor. A summary of the calibration gases used is provided in Table 2-1. The calibration gases were obtained from Mesa Specialty Gases & Equipment.

Table 2-1. Composition of Calibration Gases

Lot #	H$_2$ Vol%	N$_2$O Vol%	Balance
1-130-2	0.50	9.90	Air
1-127-7	1.50	9.90	Air
1-127-6	3.00	5.00	N$_2$

2.4 <u>Test Matrix</u>

Data from previous laboratory dissolution experiments to define the MTR flowsheet was used to examine the range of off-gas compositions seen in a typical dissolution.[2] These laboratory-scale experiments measured the off-gas composition and generation rates during dissolution of Al 1100 alloy coupons. This data was then scaled to determine off-gas generation rates for typical L-bundle dissolutions in H-Canyon. A range of compositions (with varying H$_2$ concentrations) were selected for testing to represent the changing off-gas composition seen during dissolution of ASNF. From the previously mentioned laboratory dissolution experiments, the maximum off-gas generation rate was calculated for dissolution of 6 bundles of fuel at an immersion depth of 54 inches (38.73 ft^2 bundle outer surface area). This maximum rate of 40.49 scfm was determined to occur at a dissolved aluminum concentration of 0.16 M and was comprised of the following gases: H$_2$ (2.23 scfm), NO (26.25 scfm), NO$_2$ (0.04 scfm), N$_2$O (10.93 scfm), and N$_2$ (1.05 scfm). In addition to the off-gas generated from the dissolution, the off-gas stream also includes an air purge of 40 scfm, resulting in a total off-gas rate of 80.49 scfm with the following composition: 2.77% H$_2$, 32.62% NO, 0.04% NO$_2$, 13.58% N$_2$O, 1.30% N$_2$, and 49.69% air at this point in the dissolution. The 40 scfm represents the minimum purge requirement in H-Canyon, but the purge rate is often higher. Using the same data set, two additional (lower) off-gas generation points were selected for this testing to cover a range of hydrogen concentrations from 1 to 2.8%. A summary of the feed composition test matrix is provided in Table 2-2. The feed composition for Experiment number 1 shown below represents the stage in the dissolution where the aluminum concentration is 0.03 M and the composition shown for Experiment number 2 represents the point in the dissolution when the aluminum concentration is 0.09 M. Experiment number 3 is the point in the dissolution where the maximum off-gas rate was determined to occur as discussed above (aluminum concentration of 0.16 M). The off-gas also contains small amounts of NO$_2$; however, due to the low concentrations (<1%) it was excluded from this testing to simplify the feed composition. The amount of NO$_2$ in each case was replaced with additional NO. Small amounts of oxygen and nitrogen are also produced in the off-gas, but the amounts are small relative to the air purge, and therefore these amounts were replaced with additional air. Experiments 4 and 5 were designed to determine if NO and N$_2$O have any impact on the recombination reaction.

Table 2-2. Test Matrix – Feed Composition

Experiment #	H$_2$ Vol%	NO Vol%	N$_2$O Vol%	Air Vol%
1	1.0	16.6	5.2	77.2
2	1.9	22.3	11.0	64.8
3	2.8	32.6	13.6	51.0
4	1.0	0	0	99.0
5	1.9	0	0	98.1

The HFIR fuel dissolution studies produced slightly different off-gas profiles when compared to the MTR fuel dissolutions;[1] however, the hydrogen concentrations selected for this study also bound the concentrations expected in the HFIR flowsheet. Off-gas data from bench-scale dissolutions of quarter-scale Fast Critical Assembly (FCA) cans[9] was also examined and the hydrogen concentrations expected from those dissolutions are also bounded by the test matrix defined in Table 2-2 above.

To scale the experiments to be performed on the laboratory-scale iodine reactor described in Section 2.2 to the H-Canyon iodine reactor, the residence time of the gas in the reactor was chosen as the key parameter based on chemical engineering judgement (the longer the hydrogen is in contact with the berl saddles the more opportunity it has to undergo catalytic oxidation). To determine the residence time of the off-gas in the reactor, the same data from the laboratory-scale dissolution experiments described above was utilized. Adjusting the dissolver off-gas generation rate for the temperature increase at the iodine reactor results in a flow rate of 131.9 cfm at the reactor for the maximum off-gas case described above. The H-Canyon iodine reactor bed has a height of 8.19 ft and a diameter of 1.96 ft, resulting in an empty reactor volume of 24.66 ft^3.[10] The reactor is packed with 0.5-inch berl saddles resulting in a packed bed porosity of 60% or 14.8 ft^3 of void volume.[11] Using the flow rate of 131.9 cfm through the void volume in the reactor results in a residence time of 6.7 seconds for the gas in the reactor. This residence time was used to determine the flow rate of gases needed to achieve the same residence time in the laboratory-scale reactor. Similar calculations were performed for the off-gas rates containing 1% and 1.9% H$_2$ and a summary of the results is provided in Table 2-3 and Table 2-4. In addition, the residence times were varied from 0.5X to approximately 5X of the calculated residence time.[a] A summary of the full test matrix performed can be found in Appendix B.

Table 2-3. Calculated Off-Gas Residence Times

% H$_2$ of Total Off-Gas	Max. Off-Gas from System (ft^3/min) at 60 °F (15.5 °C), 1 atm	Max. Off-Gas from System (ft^3/min) at 392 °F (200 °C), 1 atm	Off-Gas Residence Time in Bed (sec)
1.0	52.7	86.4	10
1.9	64.2	105.2	8.4
2.8	80.5	131.9	6.7

Table 2-4. Scaled Flow Rates for Lab-Scale Reactor

% H$_2$ of Total Off-Gas	Scaled Flow Rate (L/min) at 60 °F (15.5 °C), 1 atm	Scaled Flow Rate (L/min) at 392 °F (200 °C), 1 atm	Off-Gas Residence Time in Bed (sec)
1.0	0.33	0.53	10
1.9	0.40	0.64	8.4
2.8	0.51	0.81	6.7

2.5 Performance of Experiments

A DACS was used to control gas flow rates with the mass flow controllers. In addition, the DACS was used to record readings from the thermocouples and mass flow controllers throughout the experiments. Prior to starting experiments the furnaces were allowed to heat to the set temperature with only air flowing through the system. Once the desired temperature was achieved in the reactor bed, the gas flow rates were set, and the hydrogen concentration in the feed was measured using the GC. Prior to beginning analysis on the GC, the slip stream line for the feed was purged for several minutes before connecting to the instrument. For each GC measurement a total of seven, 2-minute runs were performed, and the last 5 results were averaged to obtain a single average value for each experiment. After completing analysis of the feed stream, the valves were switched to pull a slip stream from the reactor outlet to the GC. Again, the line was purged for several minutes after switching the valves, prior to connection to the GC. Seven 2-minute runs were also performed on the outlet stream, again averaging the last 5 results to obtain a single value for each experiment. After collecting data for both the inlet and outlet streams, the gas flow rates were adjusted for the next experiment. Experiments were first performed with the reactor packed with uncoated berl saddles. After completion of the experiments with the uncoated saddles, the reactor was emptied and reloaded with

---

[a] Within the limits of achievable gas flows with the mass flow controllers used.

the silver nitrate-coated berl saddles for the next set of experiments. The GC was calibrated at the start of each day, and a closing calibration check was performed at the end of each day.[8]

2.6 Quality Assurance

Requirements for performing reviews of technical reports and the extent of review are established in manual E7 2.60. SRNL documents the extent and type of review using the SRNL Technical Report Design Checklist contained in WSRC-IM-2002-00011, Rev. 2.[12] This work was performed following the applicable Task Technical and Quality Assurance Plan (TTQAP).[13] The Technical Task Request (TTR) associated with this work[14] requested a functional classification of Safety Significant (see section 9.5 of the TTQAP entitled "Clarification of Safety Significant Functional Classification"). To meet the requested functional classification requirements, this report and calculations within received a technical review by design verification.[15] Data are recorded in the Electronic Laboratory Notebook (ELN) system.[16]

A DACS software package was used to display and log test readings from mass flow controllers and thermocouples. The software was also used to control the mass flow controllers based on the input gas flow rates for NO, N_2O, plant air, and hydrogen. The software name is Labview by NI[TM], Version 2014, H2 Recombination in Iodine Reactors from National Instruments, and its classification is Level D. The approved classification Document No. is B-SWCD-A-00741.[17] The DACS software displays the temperature and mass flow rates and records a data file for later use. The DACS software does not perform calculations that are used in this report. The thermocouples and mass flow controllers are in the M&TE program and the GC used for measuring the hydrogen concentration is in the MS&E program; therefore, the measurements meet the requirements for Safety Significant application.

3.0 Results and Discussion

3.1 Berl Saddles

A summary of the weight gains for each batch of silver nitrate-coated berl saddles is provided in Table 3-1. The average weight increase was 11.3 wt %. The silver nitrate-coated berl saddles were a shade darker than the uncoated berl saddles (Figure 3-1). The absence of a drastic color change, considering a 11.3% average mass increase, indicated the silver nitrate solution was able to permeate the porous berl saddles to make a uniform silver nitrate coating. While previous studies reported that a 5.0 wt % increase was expected,[18] those studies were also coating significantly larger batches of berl saddles. This would suggest other factors (temperature, solution volume, and residence time) significantly impact the amount of silver nitrate deposited on the berl saddles. A similar batch size of uncoated berl saddles were dried over the same time to determine if the berl saddles were hydroscopic. The mass loss of 0.023% indicated moisture absorption is minimal to negligible.

Table 3-1. Initial (uncoated) and Final (silver nitrate-coated) Masses of Berl Saddles.

Batch	Initial Mass (g)	Final Mass (g)	Wt % Change
1	28.5997	32.0158	11.9445
2	27.5931	31.4075	13.8238
3	29.1482	32.1538	10.3114
4	28.8199	31.3036	8.6180[b]
5	29.6442	33.5563	13.1969
6	29.1685	32.4468	11.2392
7	29.307	32.6189	11.3007
8	28.8236	31.9622	10.8890
9	29.2791	32.5967	11.3310
10	29.3705	32.4993	10.6529
Average	**28.9754**	**32.2561**	**11.3307**

Figure 3-1. Photograph of uncoated (as received) berl saddles (left) and berl saddles after coating with silver nitrate (right).

3.2 GC Calibration

As described in Section 2.3, the GC was calibrated each day using NIST traceable calibration gases with three different hydrogen concentrations, 0.5%, 1.5%, and 3% H_2. Figure 3-2 shows an example chromatogram from Column A of the three calibration gases with retention times of approximately 35 seconds for hydrogen, approximately 42 seconds for oxygen, and approximately 52 seconds for nitrogen. The area under the H_2 peak was used for constructing the calibration curve. The calibration curve obtained each day was used for calculating the measured hydrogen concentration in samples run that day. A closing calibration check was also performed each day with one calibration gas, and the results were always within 5% of the value obtained at the start of the day. A plot of the calibration curves obtained each day is provided in Figure 3-3. As can be seen the peak area correlates extremely well to the hydrogen concentration giving linear calibration curves. In each case the intercept was forced through zero, as a zero response would be expected in the absence of hydrogen. The closing calibration checks are shown as open

---

[b] Silver nitrate dipping solution was slightly over-diluted just prior to coating batch 4 resulting in the lower weight gain for this batch.

data points and were not included in the linear regression. The analytical error in the GC measurements was determined by calculating the percent relative standard deviation of the response factors (area/concentration) for all three calibration gases, using a total of 77 data points collected over a period of three days. The average response factor for hydrogen was 32,247 with a relative standard deviation of 2.1%.
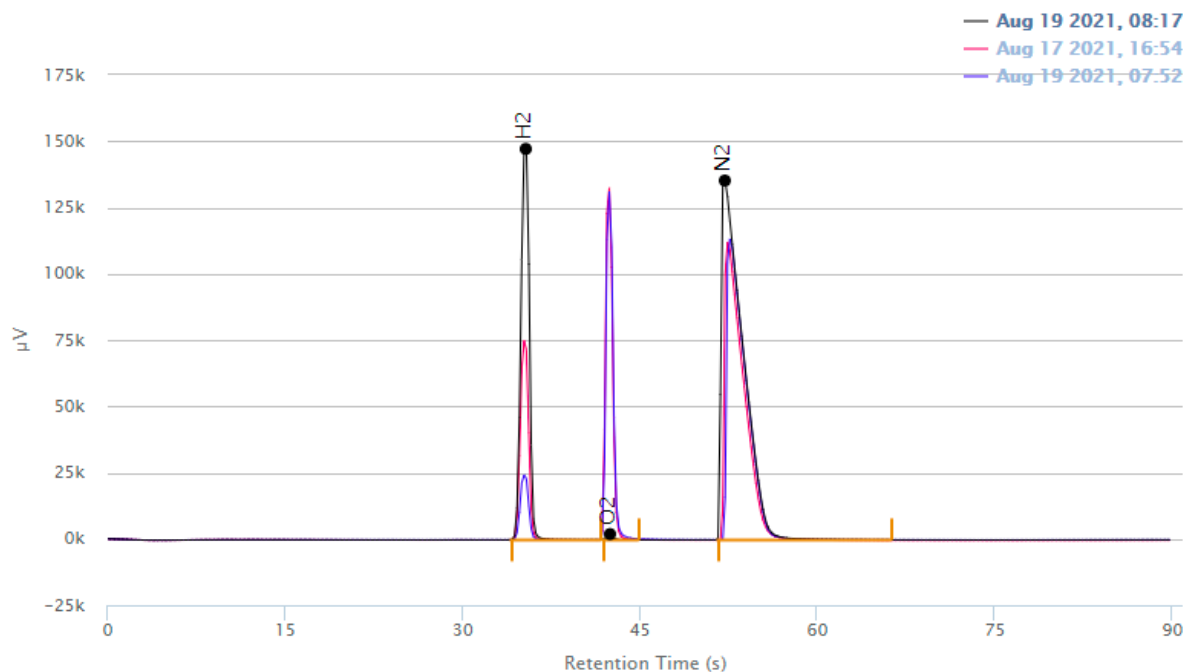
Figure 3-2. Chromatogram of calibration gases on Column A (0.5% H$_2$ in blue, 1.5% H$_2$ in pink, and 3.0% H$_2$ in black). Note the balance gas for the 3.0% H$_2$ calibration gas was nitrogen (therefore no O$_2$ peak observed) versus air as used in the 0.5% and 1.5% H$_2$ calibration gases.
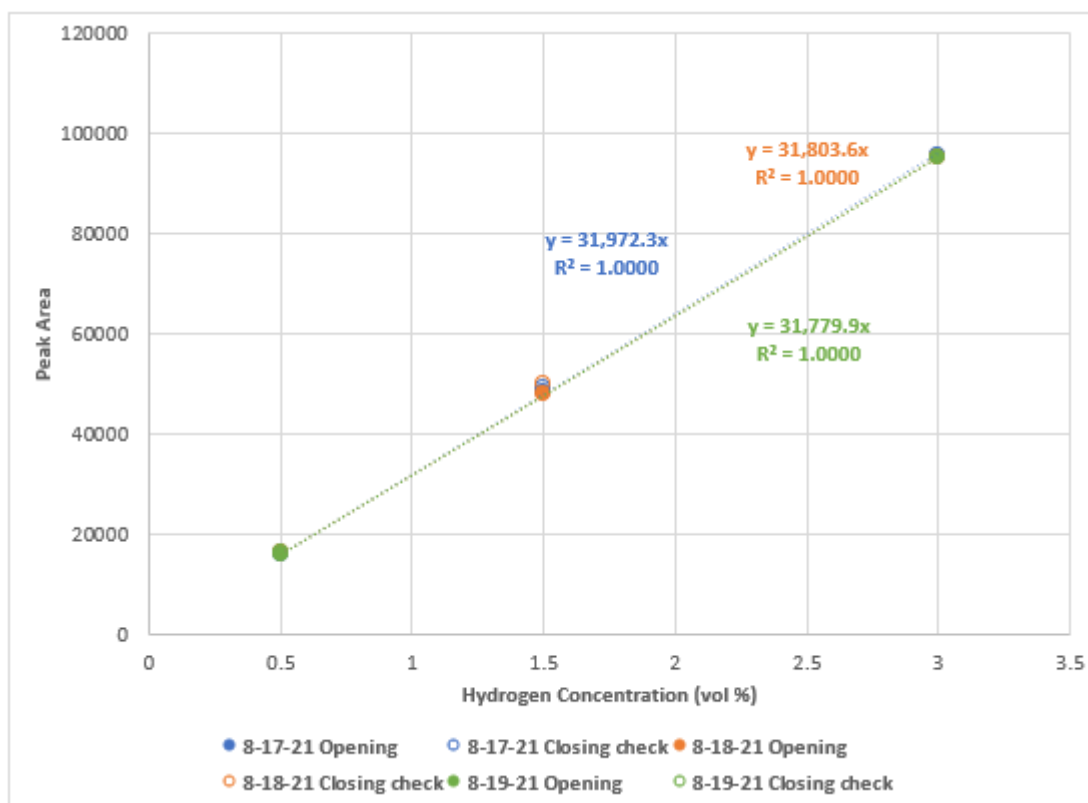
Figure 3-3. Calibration Curves for Hydrogen Measurements.

While the focus of these measurements was on hydrogen concentration, the GC is also able to detect N_2O. Using the concentrations of N_2O in the calibration gas a calibration curve for N_2O can also be constructed, although not ideal, as there are only two different N_2O concentrations in the three calibration gases. Figure 3-4 shows a portion of the chromatogram of the three calibration gases showing retention times of approximately 50-52 seconds for N_2O on column B. The area under this peak was used for constructing the calibration curve. The calibration curve obtained each day was used for calculating the measured N_2O concentration in samples run that day. A closing calibration check was also performed each day with one calibration gas, and the results were always within 2% of the value obtained at the start of the day. A plot of the calibration curves obtained each day is provided in Figure 3-5. As can be seen the peak area correlates well to the N_2O concentration, even though only two different concentrations were available for constructing the calibration curve. In each case the intercept was forced through zero, as a zero response would be expected in the absence of N_2O. The closing calibration checks are shown as open data points and were not included in the linear regression. The analytical error in the GC measurements was determined by calculating the percent relative standard deviation of the response factors (area/concentration) for all three calibration gases, using a total of 77 data points collected over a period of three days. The average response factor for N_2O was 997 with a relative standard deviation of 2.8%.
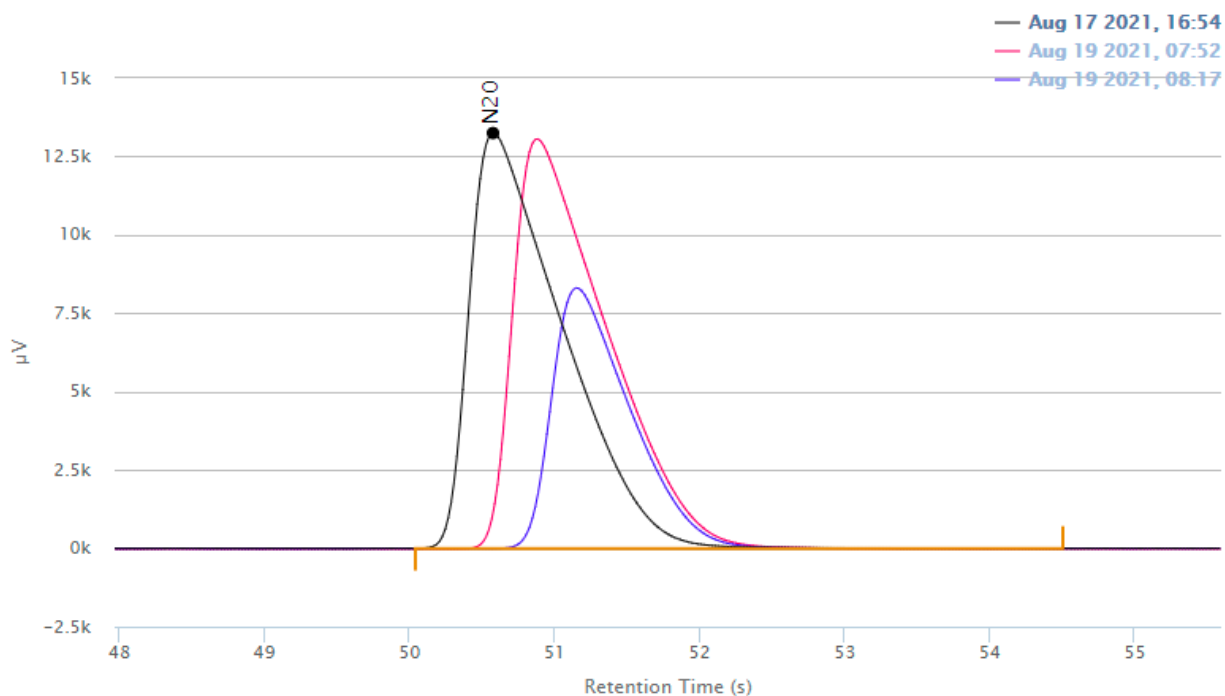
Figure 3-4. A portion of the chromatogram of calibration gases (0.5% H_2/9.9% N_2O in pink, 1.5% H_2/9.9% N_2O in black, and 3.0% H_2/5.0% N_2O in blue). Note the balance gas for the 3.0% H_2 was nitrogen versus air as used in the 0.5% and 1.5% H_2 gases.
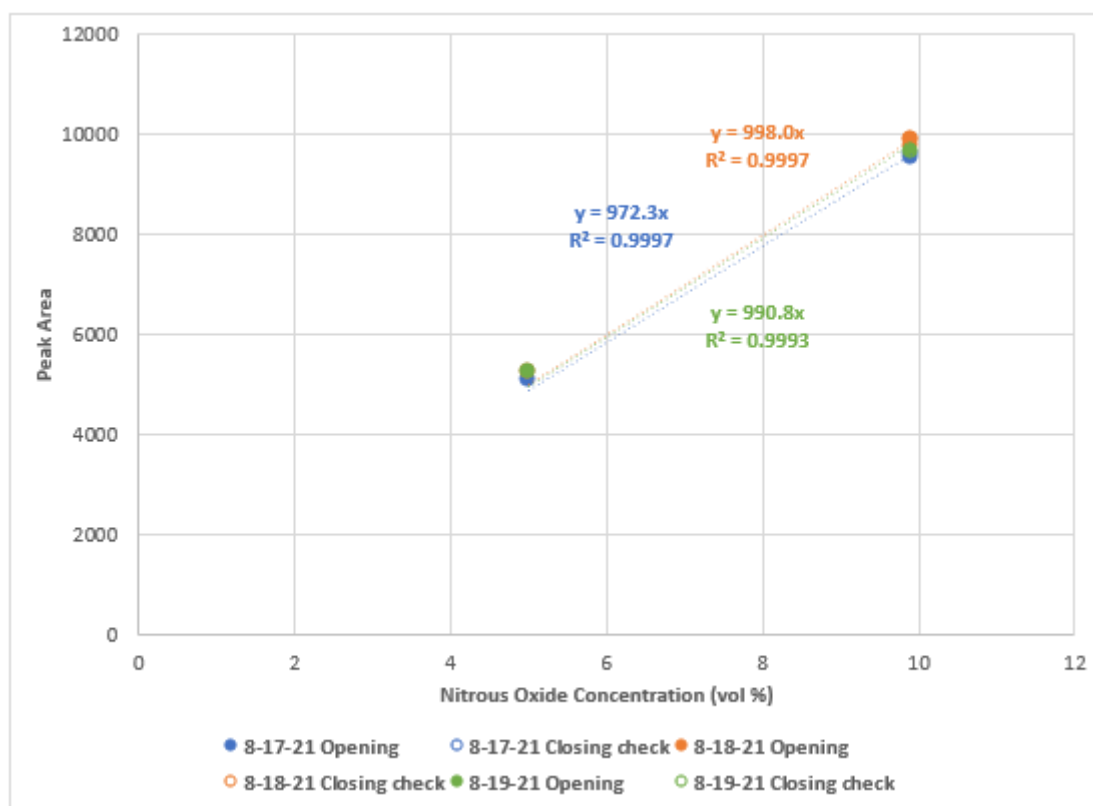
Figure 3-5. Calibration Curves for Nitrous Oxide Measurements.

3.3 Results of Testing

A summary of the results from testing with both the uncoated and coated berl saddles is provided in Table 3-2. As can be seen in each set of experiments with the uncoated berl saddles, the measured hydrogen concentration in the output stream was the same as the input (within 5%) indicating no recombination of hydrogen in the reactor bed when packed with uncoated (as received) berl saddles. In contrast, in experiments with the silver nitrate-coated berl saddles the hydrogen concentrations measured in the output streams were significantly reduced ($\geq$ 90%). All of the measured hydrogen concentrations in tests with the silver nitrate-coated berl saddles were below the concentration of the lowest standard (0.5%) requiring extrapolation of the calibration curve.

Table 3-2. Measured Hydrogen Concentrations in Experiments 1 – 5.

Test ID	Berl Saddles	Residence Time (s)	Measured H_2 Input (vol%)	Measured H_2 Output (vol%)	% H_2 Recombination
1A-UC	uncoated	10.3 (1X)	1.03	1.07	-3.42%
1A-C	Silver coated	10.3 (1X)	1.03	0.0127	98.8%
1B-C	Silver coated	20.6 (2X)	1.07	0.0122	98.9%
1C-UC	uncoated	48.9 (4.75X)	0.943	0.943	0.04%
1C-C	Silver coated	48.9 (4.75X)	1.02	0.0112	98.9%
1D-C	Silver coated	5.14 (0.5X)	1.02	0.102	90.0%
2A-UC	uncoated	8.44 (1X)	2.00	2.03	-1.90%
2A-C	Silver coated	8.44 (1X)	1.99	0.0655	96.7%
2B-C	Silver coated	16.9 (2X)	2.07	0.0178	99.1%
2C-UC	uncoated	40.9 (4.85X)	1.88	1.97	-5.01%
2C-C	Silver coated	40.9 (4.85X)	1.97	0.0162	99.2%
3A-UC	uncoated	10.1 (1.5X)	3.05	3.04	0.27%
3A-C	Silver coated	10.1 (1.5X)	2.98	0.0615	97.9%
3B-UC	uncoated	32.0 (4.75X)	2.99	3.07	-2.84%
3B-C	Silver coated	32.0 (4.75X)	2.96	0.0242	99.2%
4A-C	Silver coated	10.3 (1X)	0.971	0.0202	97.9%
4B-C	Silver coated	20.6 (2X)	0.968	3.06E-03	99.7%
4C-C	Silver coated	51.4 (5X)	1.043	9.53E-04	99.9%
4D-C	Silver coated	5.14 (0.5X)	0.964	0.0910	90.6%
5A-C	Silver coated	8.44 (1X)	1.79	0.0600	96.7%
5B-C	Silver coated	16.9 (2X)	1.85	0.0109	99.4%
5C-C	Silver coated	42.2 (5X)	1.76	2.46E-03	99.9%

Figure 3-6 shows the effect of residence time on the recombination reaction. At the shortest residence times (~5 seconds), which represents half of the expected residence time (0.5X) for the 1.0% H_2 condition, the percent recombination is still approximately 90%. However, it increases significantly from there reaching 96.7% recombination for the 8.4 second residence times; and 97.9% or greater for all residence times over 10 seconds. No correlation was found between the starting hydrogen concentration and the extent of recombination over the range tested. An example of the raw GC spectra obtained for experiments 1C-C and 1D-C (4.75X versus 0.5X residence time) is provided in Figure 3-7.
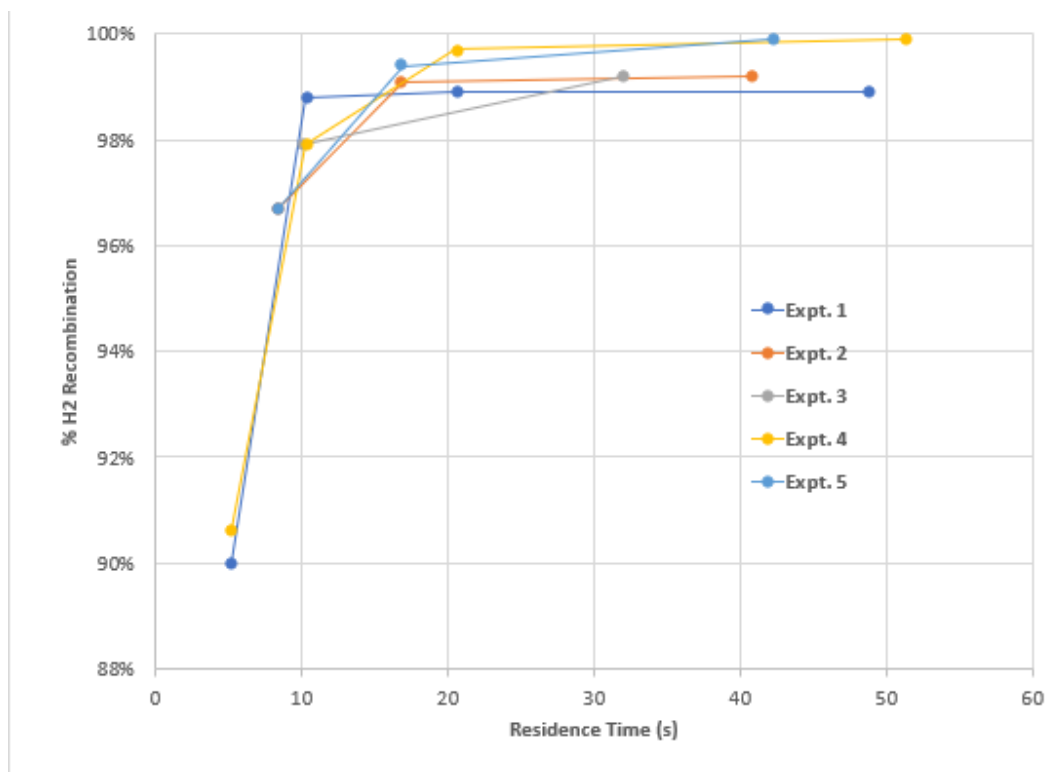
Figure 3-6. Effect of Residence Time in Reactor on the Hydrogen Recombination.
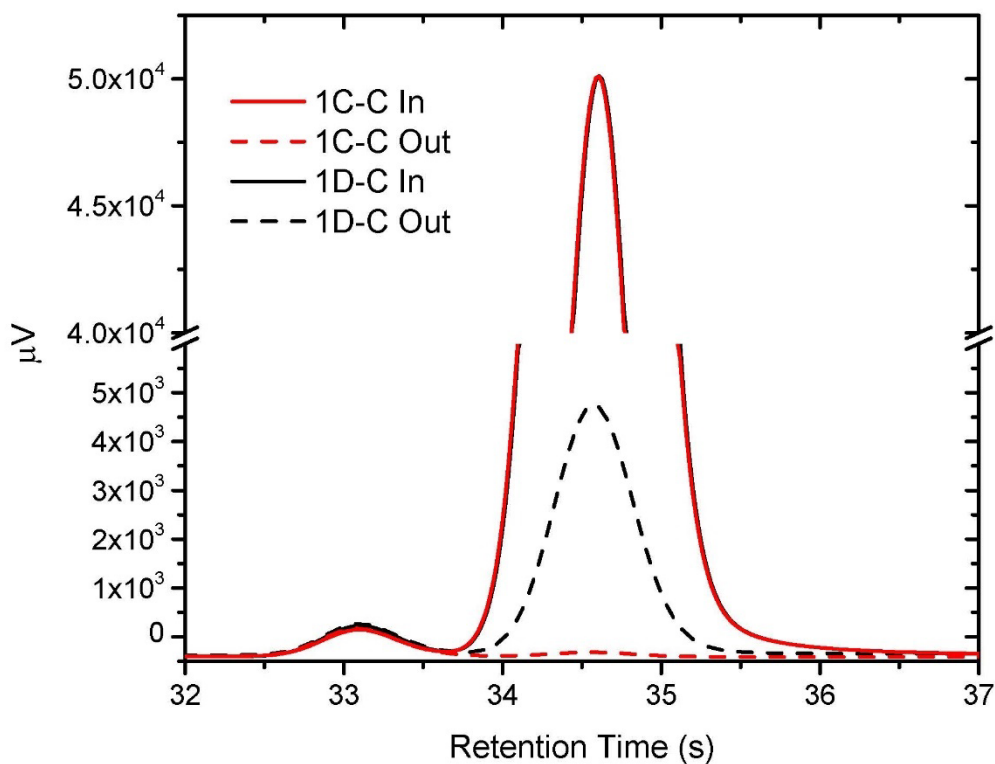
Figure 3-7. Comparison of GC spectra for experiments 1C-C and 1D-C (4.75X vs. 0.5X residence times).

Comparing experiments 1 with 4 and 2 with 5 shows the effect of the presence or absence of the NO and N_2O gases in the feed. As can be seen in Figures 3-8 and 3-9 there is not a consistent trend. For the 1.0% H_2 feed (experiments 1 and 4), it does appear the recombination is slightly higher in the absence of the NO and N_2O gases, with the exception of the 1X residence time. Similar results are also seen for the 1.9% H_2 feed (experiments 2 and 5). However, these differences are likely within the analytical uncertainty of the measurements, especially considering the low hydrogen concentrations being measured. An example GC spectra comparing experiments 2A-C and 5A-C is provided in Figure 3-10.
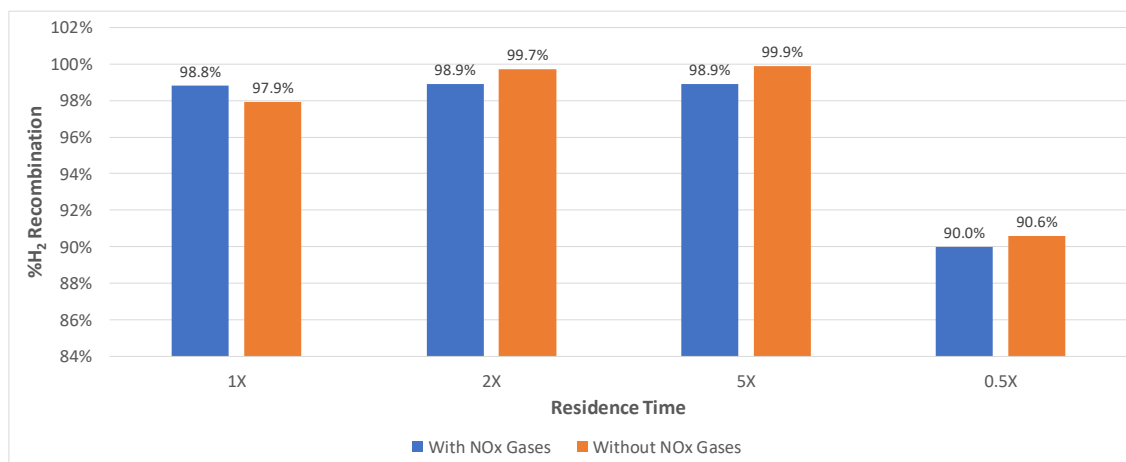
Figure 3-8. Comparison of Results from Experiments 1 and 4 with the silver nitrate-coated berl saddles (effect of the presence of NO and N_2O gases).
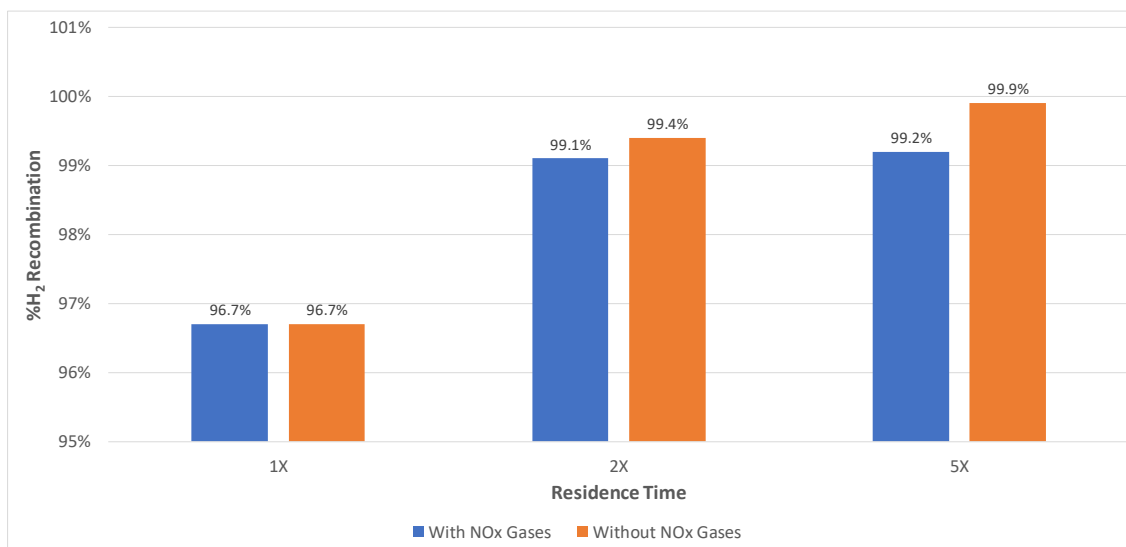
Figure 3-9. Comparison of Results from Experiments 2 and 5 with the silver nitrate-coated berl saddles (effect of the presence of NO and N_2O gases).
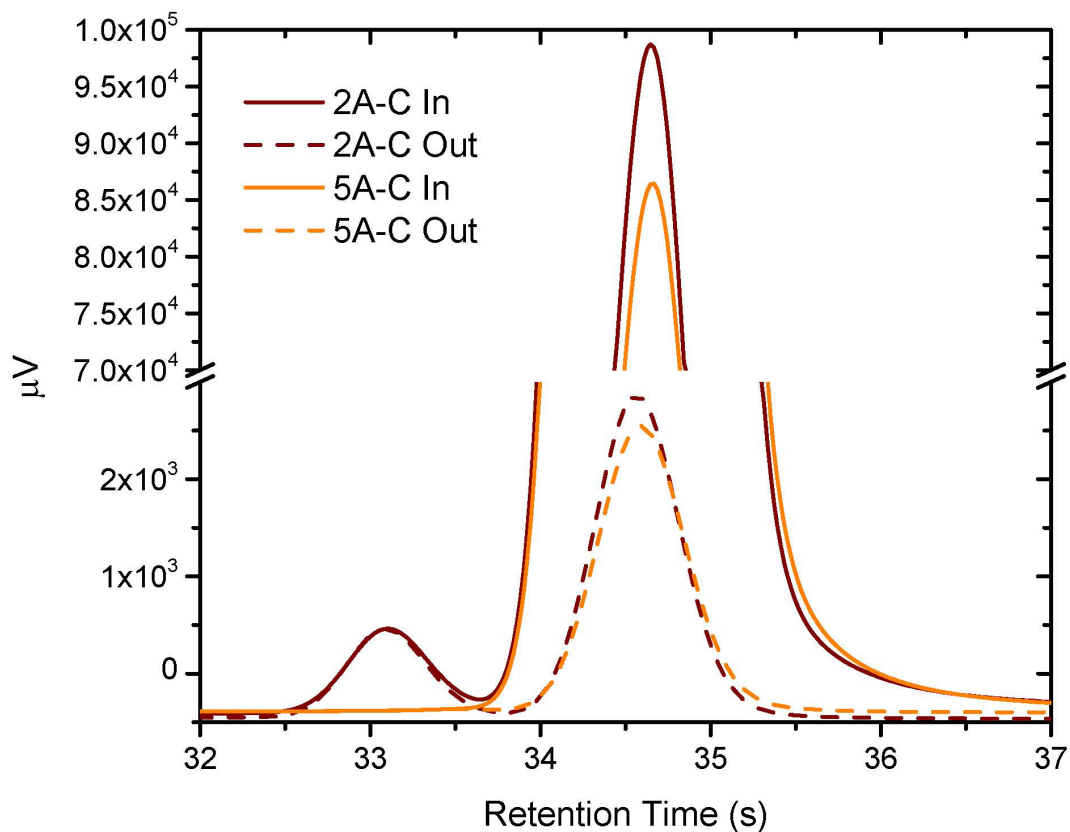
Figure 3-10. Comparison of GC spectra for experiments 2A-C and 5A-C (with and without the presence of NO and N_2O gases).

The N_2O concentration was also measured by GC, and as can be seen from the results in Table 3-3, there was no significant change (within 2-sigma uncertainty) in N_2O concentration after passing through the reactor.

Table 3-3. Nitrous Oxide Concentrations in Experiments 1 – 3.

Test ID	Berl Saddles	Residence Time (s)	Measured N_2O Input (vol%)	Measured N_2O Output (vol%)	% Change
1A-UC	uncoated	10.3 (1X)	5.85	5.89	0.746%
1A-C	Silver coated	10.3 (1X)	5.93	6.09	2.59%
1B-C	Silver coated	20.6 (2X)	5.96	6.09	2.18%
1C-UC	uncoated	48.9 (4.75X)	4.89	4.90	0.244%
1C-C	Silver coated	48.9 (4.75X)	5.76	5.98	3.93%
1D-C	Silver coated	5.14 (0.5X)	5.80	5.80	0.0222%
2A-UC	uncoated	8.44 (1X)	12.4	12.4	0.106%
2A-C	Silver coated	8.44 (1X)	12.6	12.9	2.43%
2B-C	Silver coated	16.9 (2X)	13.1	13.6	3.94%
2C-UC	uncoated	40.9 (4.85X)	11.5	12.1	5.22%
2C-C	Silver coated	40.9 (4.85X)	12.1	12.8	5.42%
3A-UC	uncoated	10.1 (1.5X)	16.7	16.4	-1.72%
3A-C	Silver coated	10.1 (1.5X)	16.4	16.3	-0.385%
3B-UC	uncoated	32.0 (4.75X)	16.0	16.7	4.58%
3B-C	Silver coated	32.0 (4.75X)	15.5	15.9	2.57%

4.0 Conclusions

To test the hypothesis that the silver nitrate-coated berl saddles present in the iodine reactor were acting as a catalytic hydrogen recombiner, a laboratory-scale reactor was assembled and filled with silver nitrate-coated berl saddles. Testing with this laboratory-scale reactor confirmed the recombination of hydrogen when a simulated dissolver off-gas was passed through the reactor containing silver nitrate-coated berl saddles. Control experiments performed with uncoated berl saddles resulted in no change to the hydrogen concentration after passing through the reactor. The expected recombination reaction is shown in Equation 8 below, where the expected product is water vapor. The water vapor was not detected by GC during the experiments as it was later found to elute beyond the collection window established for measuring the hydrogen concentration.

$$H_2 + \frac{1}{2}O_2 \xrightarrow{Ag^+} H_2O \qquad\qquad (8)$$

The residence time of the gas in the reactor was varied to determine if residence time had an impact on the amount of hydrogen recombination occurring. Results from these experiments indicated at the shortest residence times tested (~5 seconds) recombination of the hydrogen still exceeded 90%; however, the percent recombination did increase at longer residence times, reaching 97.9% or greater for residence times over 10 seconds. Therefore, there does appear to be an effect of residence time on the reaction where the recombination is reduced at very short residence times. The residence time in the reactor was determined to be the key scaling parameter for comparison between the lab-scale and facility-scale iodine reactors. Increased purge rates will result in decreased residence times in the reactor, and therefore may reduce the efficiency of the recombination reaction. Based on data obtained during analysis of the off-gas stream during dissolution with a Raman spectrometer, it appears that the residence times in the facility are sufficient to allow for the recombination reaction to take place resulting in no H_2 being detected.[5] This data also suggests that the capture of iodine on the silver nitrate coated saddles does not interfere with the recombination reaction, at least not at the current iodine loading levels.

Finally, testing performed with a simplified off-gas composition containing only hydrogen and air gave similar results, indicating that the presence of NO and N_2O gases in the stream do not play a role in the recombination reaction.

5.0 Recommendations

Additional testing is recommended using the laboratory reactor set-up, replacing the gas chromatograph with a Raman spectrometer. GC was selected for this work as the focus was on hydrogen; however, since the Raman spectrometer installed to monitor the H-Canyon off-gas is only detecting NO_2 it would be beneficial to perform similar measurements on the lab scale set-up to determine the fate of the NO, which is not measurable via GC. It is likely that the NO is quickly oxidized to NO_2 in the presence of oxygen, and Raman spectroscopy measurements would allow for confirmation of this reaction.

An additional recommendation is to relocate the Raman spectrometer sampling point on the H-Canyon off-gas system to a point prior to the iodine reactor in order to be able to monitor the dissolution of the MTR and HFIR fuels based on hydrogen gas generation.

6.0 References

[1] W. E. Daniel, T. S. Rudisill, P. E. O'Rourke, and N. S. Karay, "Dissolution Flowsheet for High Flux Isotope Reactor Fuel", SRNL-STI-2016-00485, Rev. 1, December 2017.

[2] W. E. Daniel, T. S. Rudisill, and P. E. O'Rourke, "Dissolution of Material Test Reactor Fuel in an H-Canyon Dissolver", SRNL-STI-2016-00725, Rev. 1, May 2018.

[3] M. L. Hyder, W. C. Perkins, M. C. Thompson, G. A. Burney, E. R. Russell, H. P. Holcomb, and L. F. Landon, "Processing of Irradiated, Enriched Uranium Fuels at the Savannah River Plant", DP-1500, April 1979.

[4] P. M. Almond, W. E. Daniel, Jr., and T. S. Rudisill, "Dissolution and Off-Gas Results for U-Al and Al Alloys Representative of MURR-Type Used Nuclear Fuels", *Sep. Sci. Technol.,* **2015**, *50*, 2790-2797.

[5] R. J. Lascola, P. E. O'Rourke, D. M. Immel, and E. Larson, "H Canyon Dissolver Offgas Monitoring Using Raman Spectroscopy", SRNL-STI-2021-00451, Rev. 0, November 2021.

[6] W. B. Watkins, "Coating of 221F dissolver off gas reactor packing with silver nitrate", March 29, 1954. Retrieved from H-Canyon Reference Library.

[7] R. H. Smith, "Procedure for coating berl saddles", September 1967. Retrieved from H-Canyon Reference Library.

[8] Manual L33, Procedure 231, Rev. 0, "Calibration and Operation of Inficon Fusion Micro Gas Chromatographs", April 21, 2020.

[9] T. T. Truong and R. E. Fuentes, "Bench-Scale Electrolytic Dissolution of Quarter-Scale FCA Cans", SRNL-STI-2020-00386, Rev. 0, October 2020.

[10] M. W. Sapp, "Off Gas Heater Reactor Cartridge & Cover Details" Drawing D186285, June 13, 1985.

[11] M. S. Peters and K. D. Timmerhaus, "Plant Design and Economics for Chemical Engineers" 3rd. ed. McGraw-Hill Book Company, New York, 1980.

[12] "Savannah River National Laboratory Technical Report Design Check Guidelines" WSRC-IM-2002-00011, Rev. 2, August 2004.

[13] K. M. L. Taylor-Pashow, M. L. Restivo, W. E. Daniel, T. S. Rudisill, J. Gogolski, and J. M. Pareizs, "Task Technical and Quality Assurance Plan for Recombination of Hydrogen in the Iodine Reactors", SRNL-RP-2021-00461, Rev. 0, April 2021.

[14] W. H. Clifton, "Recombination of Hydrogen in the Iodine Reactors", NMMD-HTS-2021-3469, Rev. 0, January 2021.

[15] Savannah River Site Manual E7 "Conduct of Engineering", Procedure 2.60 Rev. 18 "Technical Reviews", December 2, 2019.

[16] SRNL Electronic Laboratory Notebook numbers E7518-00472-04 and K8230-00479-04.

[17] M. L. Restivo, "H2 Recombination in Iodine Reactors Data Acquisition System", B-SWCD-A-00741, Rev. 1, April 2021.

[18] A. N. Parkes, "Silver Nitrate Coating of Unglazed Ceramic Berl Saddles for use in Iodine Reactors – RTA 512-S". February 3, 1970. Retrieved from H-Canyon Reference Library.

Appendix A. Equipment List

Table A-1. Mass Flow Controllers

M&TE #	Flow Rate Range	Gas	Calibration Temperature	Experiments
36548	0 – 500 sccm	NO	0 °C	All
45116	0 – 500 sccm	N_2O	70 °F	All
33032	0 – 10 sccm	H_2	70 °F	All
33036	0 – 5,000 sccm	Air	70 °F	Uncoated Saddles
36220	0 – 5,000 sccm	Air	70 °F	Coated Saddles[a]

[a]Mass flow controller used for air was replaced at start of coated saddle testing due to failure to control at low flow rates.

Table A-2. Thermocouples

M&TE #	Type	Sheath Material	Position	Experiments
46376	K	304 Stainless Steel	Inlet	All
37101	K	304 Stainless Steel	Between furnaces	All
52565	K	304 Stainless Steel	Reactor Bed	Uncoated Saddles
43567	K	304 Stainless Steel	Reactor Bed	Coated Saddles[a]
37065	K	304 Stainless Steel	Outlet	All

[a]Thermocouple in reactor bed was broken during change out of berl saddles. Replaced with new thermocouple for testing with the coated saddles.

Table A-3. GC

MS&E #	Vendor	Model Number	Experiments
43279	Inficon Fusion	F08180UC2TR2	All

Appendix B. Summary of Experimental Conditions

Table B-1. Test Matrix – Uncoated Berl Saddles.

Test ID	H₂ Vol.%	Residence Time (s)	Target Flow Rates (mL/min)				Cumulative Flow Rate (L/min)
			Air	N₂O	NO	H₂	
1A-UC	1.0	10.3 (1X)	257	17.3	55.2	3.32	0.33
1C-UC	1.0	48.9 (4.75X)	54.0	3.64	11.6	0.700	0.07
2A-UC	1.9	8.44 (1X)	262	44.5	90.2	7.69	0.40
2C-UC	1.9	40.9 (4.85X)	54.1	9.18	18.6	1.59	0.08
3A-UC	2.8	10.1 (1.5X)	173	46.0	110	9.48	0.34
3B-UC	2.8	32.0 (4.75X)	54.5	14.5	34.8	2.99	0.11

Table B-2. Test Matrix – Silver Nitrate Coated Berl Saddles.

Test ID	H₂ Vol.%	Residence Time (s)	Target Flow Rates (mL/min)				Cumulative Flow Rate (L/min)
			Air	N₂O	NO	H₂	
1A-C	1.0	10.3 (1X)	257	17.3	55.2	3.32	0.33
1B-C	1.0	20.6 (2X)	128	8.64	27.6	1.66	0.17
1C-C	1.0	48.9 (4.75X)	54.0	3.64	11.6	0.700	0.07
1D-C	1.0	5.14 (0.5X)	513	34.6	110	6.65	0.66
2A-C	1.9	8.44 (1X)	262	44.5	90.2	7.69	0.40
2B-C	1.9	16.9 (2X)	131	22.3	45.1	3.84	0.20
2C-C	1.9	40.9 (4.85X)	54.1	9.18	18.6	1.59	0.08
3A-C	2.8	10.1 (1.5X)	173	46.0	110	9.48	0.34
3B-C	2.8	32.0 (4.75X)	54.5	14.5	34.8	2.99	0.11
4A-C	1.0	10.3 (1X)	329	0	0	3.32	0.33
4B-C	1.0	20.6 (2X)	165	0	0	1.66	0.17
4C-C	1.0	51.4 (5X)	65.8	0	0	0.665	0.07
4D-C	1.0	5.14 (0.5X)	658	0	0	6.65	0.66
5A-C	1.9	8.44 (1X)	397	0	0	7.69	0.40
5B-C	1.9	16.9 (2X)	198	0	0	3.84	0.20
5C-C	1.9	42.2 (5X)	79.4	0	0	1.54	0.08

Table B-3.   Experimental Conditions for Experiment 1.

Test ID	Berl Saddles	Input/ Output	Avg. Bed Temp. (°C)	Avg. H_2 Flow Rate (mL/min)	Avg. Air Flow Rate (mL/min)	Avg. N_2O Flow Rate (mL/min)	Avg. NO Flow Rate (mL/min)
1A-UC	uncoated	Input	176.2 (0.04%RSD)	3.31 (0.12%RSD)	245 (0.60%RSD)	17.2 (1.49%RSD)	59.3 (0.39%RSD)
1A-UC	uncoated	Output	172.4 (0.32%RSD)	3.31 (0.16%RSD)	245 (0.60%RSD)	17.1 (0.94%RSD)	59.3 (0.32%RSD)
1C-UC	uncoated	Input	176.9 (0.03%RSD)	0.686 (0.55%RSD)	50.5 (2.92%RSD)	3.28 (4.95%RSD)	12.8 (0.00%RSD)
1C-UC	uncoated	Output	177.1 (0.13%RSD)	0.687 (0.00%RSD)	51.5 (4.57%RSD)	3.26 (5.85%RSD)	12.8 (0.00%RSD)
1A-C	Silver coated	Input	181.1 (0.05%RSD)	3.32 (0.15%RSD)	256 (0.69%RSD)	17.3 (0.38%RSD)	59.7 (0.00%RSD)
1A-C	Silver coated	Output	180.1 (0.10%RSD)	3.32 (0.15%RSD)	256 (0.84%RSD)	17.3 (0.24%RSD)	59.7 (0.00%RSD)
1B-C	Silver coated	Input	182.3 (0.04%RSD)	1.68 (0.26%RSD)	125 (1.26%RSD)	8.63 (0.42%RSD)	29.7 (0.78%RSD)
1B-C	Silver coated	Output	181.9 (0.03%RSD)	1.67 (0.30%RSD)	125 (1.20%RSD)	8.64 (0.38%RSD)	29.8 (0.54%RSD)
1C-C	Silver coated	Input	181.8 (0.08%RSD)	0.71 (0.50%RSD)	55.0 (0.00%RSD)	3.65 (0.99%RSD)	12.4 (2.04%RSD)
1C-C	Silver coated	Output	182.6 (0.08%RSD)	0.71 (0.00%RSD)	55.5 (2.65%RSD)	3.65 (0.96%RSD)	12.4 (2.04%RSD)
1D-C	Silver coated	Input	179.4 (0.17%RSD)	6.66 (0.08%RSD)	518 (0.49%RSD)	34.6 (0.13%RSD)	118 (0.13%RSD)
1D-C	Silver coated	Output	178.8 (0.03%RSD)	6.66 (0.07%RSD)	517 (0.49%RSD)	34.6 (0.12%RSD)	118 (0.10%RSD)

Table B-4. Experimental Conditions for Experiment 2.

Test ID	Berl Saddles	Input/ Output	Avg. Bed Temp. (°C)	Avg. H_2 Flow Rate (mL/min)	Avg. Air Flow Rate (mL/min)	Avg. N_2O Flow Rate (mL/min)	Avg. NO Flow Rate (mL/min)
2A-UC	uncoated	Input	175.7 (0.02%RSD)	7.74 (0.06%RSD)	263 (0.92%RSD)	44.4 (0.26%RSD)	97.0 (0.19%RSD)
2A-UC	uncoated	Output	174.6 (0.34%RSD)	7.74 (0.06%RSD)	264 (0.86%RSD)	44.4 (0.29%RSD)	96.9 (0.24%RSD)
2C-UC	uncoated	Input	177.5 (0.11%RSD)	1.56 (0.25%RSD)	52.3 (4.87%RSD)	9.07 (1.14%RSD)	19.9 (1.22%RSD)
2C-UC	uncoated	Output	178.0 (0.02%RSD)	1.56 (0.27%RSD)	50.2 (2.08%RSD)	9.07 (1.03%RSD)	19.9 (1.30%RSD)
2A-C	Silver coated	Input	181.7 (0.02%RSD)	7.70 (0.06%RSD)	267 (0.89%RSD)	44.5 (0.11%RSD)	97.6 (0.12%RSD)
2A-C	Silver coated	Output	181.7 (0.02%RSD)	7.70 (0.07%RSD)	267 (0.89%RSD)	44.5 (0.11%RSD)	97.6 (0.00%RSD)
2B-C	Silver coated	Input	182.2 (0.03%RSD)	3.83 (0.06%RSD)	125 (1.20%RSD)	22.3 (0.20%RSD)	48.8 (0.55%RSD)
2B-C	Silver coated	Output	182.5 (0.01%RSD)	3.83 (0.09%RSD)	125 (0.85%RSD)	22.3 (0.23%RSD)	48.9 (0.50%RSD)
2C-C	Silver coated	Input	183.1 (0.02%RSD)	1.58 (0.32%RSD)	55.0 (2.87%RSD)	9.15 (0.23%RSD)	20.1 (1.16%RSD)
2C-C	Silver coated	Output	182.6 (0.04%RSD)	1.58 (0.32%RSD)	54.8 (1.95%RSD)	9.13 (0.38%RSD)	20.2 (0.93%RSD)

Table B-5. Experimental Conditions for Experiment 3.

Test ID	Berl Saddles	Input/ Output	Avg. Bed Temp. (°C)	Avg. H_2 Flow Rate (mL/min)	Avg. Air Flow Rate (mL/min)	Avg. N_2O Flow Rate (mL/min)	Avg. NO Flow Rate (mL/min)
3A-UC	uncoated	Input	176.1 (0.11%RSD)	9.53 (0.05%RSD)	169 (1.35%RSD)	46.2 (0.30%RSD)	118 (0.18%RSD)
3A-UC	uncoated	Output	176.3 (0.32%RSD)	9.44 (0.05%RSD)	173 (1.48%RSD)	46.0 (0.19%RSD)	118 (0.16%RSD)
3B-UC	uncoated	Input	176.4 (0.07%RSD)	2.98 (0.13%RSD)	51.8 (4.75%RSD)	14.4 (0.58%RSD)	37.3 (0.00%RSD)
3B-UC	uncoated	Output	176.2 (0.03%RSD)	2.98 (0.12%RSD)	50.5 (2.98%RSD)	14.4 (1.14%RSD)	37.3 (0.00%RSD)
3A-C	Silver coated	Input	180.6 (0.05%RSD)	9.50 (0.04%RSD)	176 (1.12%RSD)	46.1 (0.09%RSD)	118 (0.16%RSD)
3A-C	Silver coated	Output	181.4 (0.08%RSD)	9.49 (0.03%RSD)	175 (0.84%RSD)	46.0 (0.08%RSD)	118 (0.13%RSD)
3B-C	Silver coated	Input	182.6 (0.06%RSD)	2.98 (0.17%RSD)	55.0 (0.00%RSD)	14.5 (0.29%RSD)	37.5 (0.71%RSD)
3B-C	Silver coated	Output	182.6 (0.04%RSD)	2.98 (0.15%RSD)	55.5 (2.65%RSD)	14.5 (0.39%RSD)	37.4 (0.61%RSD)

Table B-6. Experimental Conditions for Experiment 4.

Test ID	Berl Saddles	Input/ Output	Avg. Bed Temp. (°C)	Avg. H_2 Flow Rate (mL/min)	Avg. Air Flow Rate (mL/min)
4A-C	Silver coated	Input	176.9 (0.08%RSD)	3.31 (0.15%RSD)	327 (0.74%RSD)
4A-C	Silver coated	Output	176.8 (0.07%RSD)	3.31 (0.15%RSD)	328 (0.78%RSD)
4B-C	Silver coated	Input	178.2 (0.08%RSD)	1.66 (0.29%RSD)	166 (1.29%RSD)
4B-C	Silver coated	Output	178.7 (0.02%RSD)	1.66 (0.26%RSD)	166 (1.06%RSD)
4C-C	Silver coated	Input	179.2 (0.04%RSD)	0.667 (0.47%RSD)	61.6 (3.87%RSD)
4C-C	Silver coated	Output	179.5 (0.02%RSD)	0.667 (0.32%RSD)	60.9 (3.24%RSD)
4D-C	Silver coated	Input	176.4 (0.23%RSD)	6.66 (0.05%RSD)	658 (0.38%RSD)
4D-C	Silver coated	Output	174.6 (0.13%RSD)	6.66 (0.08%RSD)	658 (0.39%RSD)

Table B-7. Experimental Conditions for Experiment 5.

Test ID	Berl Saddles	Input/ Output	Avg. Bed Temp. (°C)	Avg. H_2 Flow Rate (mL/min)	Avg. Air Flow Rate (mL/min)
5A-C	Silver coated	Input	176.3 (0.15%RSD)	7.69 (0.07%RSD)	398 (0.64%RSD)
5A-C	Silver coated	Output	177.2 (0.04%RSD)	7.69 (0.06%RSD)	397 (0.64%RSD)
5B-C	Silver coated	Input	178.4 (0.06%RSD)	3.84 (0.13%RSD)	196 (1.01%RSD)
5B-C	Silver coated	Output	178.9 (0.03%RSD)	3.84 (0.11%RSD)	196 (0.90%RSD)
5C-C	Silver coated	Input	179.1 (0.02%RSD)	1.53 (0.32%RSD)	80.9 (2.44%RSD)
5C-C	Silver coated	Output	179.1 (0.03%RSD)	1.53 (0.30%RSD)	80.7 (2.18%RSD)

Distribution:

cj.bannochie@srnl.doe.gov
William.bates@srnl.doe.gov
marion.cofer@srnl.doe.gov
alex.cozzi@srnl.doe.gov
connie.herman@srnl.doe.gov
brady.lee@srnl.doe.gov
Joseph.Manna@srnl.doe.gov
Gregg.Morgan@srnl.doe.gov
frank.pennebaker@srnl.doe.gov
William.Ramsey@SRNL.DOE.gov
Marissa.Reigel@srnl.doe.gov
eric.skidmore@srnl.doe.gov
michael.stone@srnl.doe.gov
william.swift@srnl.doe.gov
Boyd.Wiedenman@srnl.doe.gov
lance.traver@srnl.doe.gov
eddie.kyser@srnl.doe.gov
joy.mcnamara@srnl.doe.gov
kathryn.taylor-pashow@srnl.doe.gov
michael.restivo@srnl.doe.gov
jarrod.gogolski@srnl.doe.gov
john.pareizs@srnl.doe.gov
gene.daniel@srnl.doe.gov
tracy.rudisill@srnl.doe.gov
harris.eldridge@srnl.doe.gov
jonathan.duffey@srnl.doe.gov
Catherine.Mussi@srnl.doe.gov
David.Herman@srnl.doe.gov
patrick.o'rourke@srnl.doe.gov
robert.lascola@srnl.doe.gov

steven.brown@srs.gov
brett.clinton@srs.gov
james.therrell@srs.gov
kenneth.burrows@srs.gov
kevin.usher@srs.gov
tara.smith@srs.gov
bill.clifton@srs.gov
nina.smith@srs.gov
mark.hudlow@srs.gov
jaclyn.fitzpatrick@srs.gov
omar.rodriquez@srs.gov
matthew.arnold@srs.gov
mackenzie.yerger@srs.gov
robert.gunby@srs.gov

Records Administration (EDWS)